Ab Initio Hartree−Fock Study of Brønsted Acidity at the Surface of Oxides

P. Nortier*

Service de Synthèse Minérale, Rhône-Poulenc Recherches, 52 rue de la Haie-Coq, 93308 Aubervilliers Cedex, France

A. P. Borosy[†] **and M. Allavena**

Laboratoire de Chimie Théorique (UPR 9070 CNRS), Université Pierre et Marie Curie, 4 Place Jussieu, 75252 Paris Cedex 05, France

Received: July 26, 1996; In Final Form: November 22, 1996[⊗]

Ab initio calculations using small sets of basis functions and pseudopotentials within the framework of the cluster model have been applied to the determination of a scale of acidity at oxide surfaces. Results are compared with available experimental data and correlated to values deduced from semiempirical models. A fair agreement between the series of data supports the validity of local models for evaluating acidic properties on oxide surfaces. The acidity of the surface sites of oxides is driven by the electrostatics of the system and is mainly governed by three structural parameters: the coordination number of the hydroxyl group, the charge on the cation(s), and the coordination number of the cation(s).

Introduction

The determination of acidity in homogeneous aqueous solution or in the gas phase is currently an almost routine measurement and does not create major problems of interpretation. However, the situation is entirely different with regard to solid surfaces.

In the case of solid−gas interfaces, all acidity measurements are indirect using (i) adsorption and thermodesorption, (ii) nuclear magnetic resonance, (iii) positron annihilation, (iv) atomic force microscopy or, (v) infrared spectroscopy by reflectance. None of these methods yields quantitative energetics. The dependence of acid−base properties of indicators on the adsorption or the global character of test reactions is a source of difficulty when attempting to determine a scale of acidity.

Similarly, classical titration in water appears to be questionable when involving solids, since adsorption of charged species on the surface creates an electrostatic potential which in turn modifies the equilibrium. In addition, a solid surface may be composed of a distribution of sites, each one having a specific structure and acidity strength. As a result, simulating titration curves on surfaces requires models containing many parameters to characterize double-layer capacitance and thickness as well as several acidity constants (pK_a's). In addition, when considering the many sources of error due to titration of suspensions (such as agglomeration), it must be stressed that the so called "experimental" pK_a's deduced from measurements on solids are far from being reliable, a fact which is confirmed by considering the dispersion of data published in the current literature.

This lack of reliable data and the need for rationalizing experimental trends observed in solids, especially oxides, in catalysis or colloid science has given rise to many phenomenological models, each one focusing attention on some specific features or parameters like Fermi level, formal charges, electronegativity, radius, or ionization potential of cations. In this connection, two recently proposed models merit special attention: (i) the multisite complexation model of T. Hiemstra et al. (MUSIC)[1] and (ii) the structure dependant partial charge model of M. Henry.[2] They are both very straightforward, and in particular, C. Contescu[3] has published experimental results on alumina that fit the predictions of MUSIC very well.

As will be discussed below, a theoretical description of chemical reactions at the solid−gas or solid−solution interface still gives rise to serious difficulties. Taking advantage of the recent development of computer facilities which allows applications of quantum chemistry methods to much larger molecular systems, the present work is intended to reinvestigate the problem of proton attachment on the surface of oxides. A better representation of the neighborhood of the hydroxyl groups, associated with good-quality Hartree−Fock calculations, should permit an acidity scale to be setup at the microscopic level. These theoretical data may also serve as reference for further comparisons with experimental results and predictions of classical models.

Method of Calculation

Model. Two possibilities are presently available for the treatment of solid materials by quantum chemistry methods: (i) a global treatment, using the periodic Hartree−Fock method,[4] and (ii) the traditional methods of quantum chemistry, particularly convenient for the calculation of local properties but whose application is restricted to a model containing a limited number of atoms (cluster) assumed to be sufficient to mimic the properties of the bulk. The energy of deprotonation requires the calculation of two sites differing by a charge of +1, which obviously implies that they cannot both be neutral. The treatment of charged species being difficult to handle efficiently with codes like CRYSTAL or EMBED,[5] the present work has been limited to the use of the cluster model. This approach has been successfully used in zeolithes[6−8] and to a lesser extent in other systems (aluminas,[9,10] titania,[11] sulfated zirconia,[12] magnesia[13]).

Cluster building rests on very simple principles consisting of admitting that all significant interactions can be evaluated by restricting calculations to the site of interest (here the acidic OH group) surrounded by one or several shells of nearest neighboring atoms (or molecules).

* Corresponding author.
† Present address: Gyogyszerkutato Intezet, Budapest, Berlini ut 45-47. 1045, Hungary.
⊗ Abstract published in *Advance ACS Abstracts,* January 15, 1997.

S1089-5647(96)02263-8 CCC: $14.00

However, for metal oxides this procedure involves breaking covalent bonds between the atoms of the external cluster shell and those of the remaining bulk. Saturating the dangling bond requires that a partition rule be set up in order to redistribute the electrons between the boundary atom and the bulk of the system. Depending on this rule, the cluster may be charged or neutral and include some dangling bonds or not. Neutrality is traditionally imposed by saturating the bonds with monovalent atoms. In order to minimize the perturbation of the electronic density of the original system, these atoms should have an electronegativity close to that of the substituted atoms or have fractional charges as in the case of δ-alumina. These healing atoms are rather easily simulated within the framework of semiempirical methods,[14] but this is not possible in the context of ab initio methods. Two strategies may be adopted: (i) Build clusters where all the bonds are naturally saturated, as is possible for some sites in α-Al_2O_3 or MgO. However, unfortunately for structural reasons this procedure is restricted to a limited number of minerals. (ii) Partition the system in such a manner that the number of dangling bonds is minimal and that cluster frontier atoms have integer charges, and then saturate these bonds with monovalent atoms as described above. Among monovalent atoms, the hydrogen atom is the usual candidate mainly because addition of an H atom adds only one electron and does not add significantly to the total basis set of the system. Clusters which are constructed in this manner allow a more complete representation of the OH group environment but are of larger size. This strategy was recommended by several authors[15] and will be adopted in the present work.

The components of the clusters were cut out graphically from the experimental bulk structures using the CERIUS[16] and INSIGHT II[17] programs. Structures were taken from the data basis provided by the programs, except for the δ- and θ-aluminas.[18]

No reconstruction of surfaces was taken into account in this study. This could be done using either the MARVIN code[19] or ab initio techniques[20] to allow relaxation before the extraction of the cluster or geometry optimization in the cluster during the calculation process. We verified in the case of the site Ia of δ-Al_2O_3 that the energy of deprotonation is modified by less than 0.01 au when the position of the cation is optimized in the course of the calculation. We can also compare sites described by the same cation, the same coordination numbers of both the hydroxyl and cation, and that differ in geometry since the materials are different (Ia in both δ- and θ-Al_2O_3, Ib in same materials, I in both anatase and rutile): the differences are rather small. This will look less surprising in regard to our conclusions: acidity is a local phenomenon, strongly depending on the coordination numbers and formal charge and weakly depending on geometry.

Work in progress includes taking into account the effect of the solid by embedding the cluster into an infinite array of charges which creates a potential at the sites of the cluster atoms. This will certainly require a better description of the actual (relaxed) surface.

The clusters were named using the classification of H. Knözinger,[21] illustrated in Figure 1, and chosen to represent the different sites identified by A. A. Tsyganenko.[22] A list of the clusters studied in the present work is given in Table 1. Perspective representations are not included since they can be misleading in the case of the most complicated systems. The optimized geometries are available from the authors as files in pdb format.

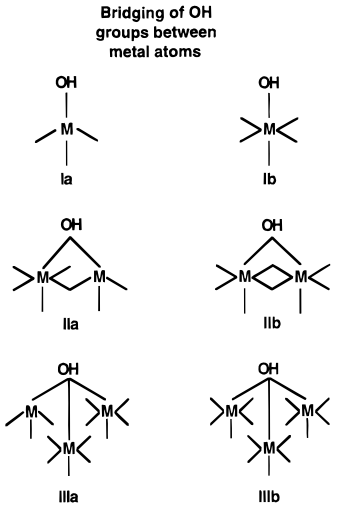

Figure 1. Nomenclature for surface sites.

TABLE 1: Stoichiometry of the Clusters

structure	face	site				
			Al	O	H	
Al_2O_3, δ	110c	Ia	1	4	5	H_4O_3AlOH
	001	Ib	1	6	9	H_8O_5AlOH
	110d	IIa	2	9	12	$H_{11}O_8Al_2OH$
	110c	IIb	2	10	14	$H_{13}O_9Al_2OH$
	110c	IIIa	3	13	17	$H_{16}O_{12}Al_3OH$
	110d	IIIb	3	13	17	$H_{16}O_{12}Al_3OH$
Al_2O_3, θ	102	I	1	4	5	H_4O_3AlOH
	102	III	3	12	15	$H_{14}O_{11}Al_3OH$
			Si	O	H	
SiO_2 (amorphous)		I	1	4	4	H_3O_3SiOH
			Ti	O	H	
TiO_2, rutile	110	I	1	6	8	H_7O_5TiOH
	110	II	2	10	12	$H_{11}O_9Ti_2OH$
	110	III	3	15	18	$H_{17}O_{14}Ti_3OH$
TiO_2, anatase	010	I	1	6	8	H_7O_5TiOH
			Sn	O	H	
SnO_2	110	I	1	6	8	H_7O_5SnOH
			Mg	O	H	
MgO	100	I	1	6	10	H_9O_5MgOH
	110	II	2	10	16	$H_{15}O_9Mg_2OH$
	111	III	3	13	20	$H_{19}O_{12}Mg_3OH$
			Ce	O	H	
CeO_2	111	I	1	8	12	$H_{11}O_7CeOH$
	100	II	2	14	20	$H_{19}O_{13}Ce_2OH$
	111	III	3	19	26	$H_{25}O_{18}Ce_3OH$

Calculations. Calculations have been performed at the Hartree−Fock (HF) level using the GAUSSIAN 92 program.[23] In order to maintain the same accuracy throughout the systems treated here, the optimal set of basis functions was determined to provide sufficient precision without taking prohibitive computer time. Small basis sets (STO-3G, 3-21G) were compared with medium size basis sets (6-31G*) as well as core potential representations in tests. Two kinds of effective core potentials were investigated: (i) the potential proposed by Hay et al.[24] (group of Los Alamos, later designated as ECP LA) and (ii) the potential derived by Dolg and co-workers[25] (Stuttgart, here noted ECP ST).

Geometry optimizations were restricted to the acid site ($-OH_2$, $-OH$, or $-O$), while the rest of the cluster was maintained as fixed in order to simulate the solid environment. Basis set superposition error (BSSE) was evaluated using the counterpoise method.

The basic quantity calculated in the present work is the deprotonation energy (E_d), defined as the amount of energy

required in the proton transfer reaction:

$$R{-}OH \rightarrow R{-}O^- + H^+ \quad (1)$$

In quantum chemistry the energy of formation of the proton is zero, and consequently E_d is calculated as the difference:

$$E_d = E(R{-}O^-) - E(R{-}OH) \quad (2)$$

This quantity is then identical to the proton affinity (PA) of the conjugate base:

$$E_d(R{-}OH) = PA(R{-}O^-) \quad (3)$$

Relations between calculated and experimental deprotonation energies have been investigated for a series of molecules where experimental information is available.

In particular, U. Fleischer[26] has studied the various terms that constitute the enthalpy of deprotonation

$$\Delta H_{gas} = \Delta E_{HF} + \Delta E_{corr} + \Delta E_{zp} + \Delta H_{th}(T) \quad (4)$$

where ΔH_{gas} is the enthalpy of deprotonation in the gas phase, ΔE_{HF} the energy of deprotonation calculated at the Hartree−Fock level (possibly including BSSE correction), ΔE_{corr} the correction for correlation, ΔE_{zp} the difference in zero-point vibrational energy, and $\Delta H_{th}(T)$ the change in thermal energy at the temperature considered. The values proposed for ΔE_{corr}, ΔE_{zp}, and $\Delta H_{th}(T)$ are of the order of −30, −30, and −5 kJ/mol, respectively. As a result, it seems reasonable to assume that ΔE_{HF} is the major contribution.

Calculation of the acidity constant in aqueous phase ("pK_a") would require determination of the change in free enthalpy during the deprotonation in water. This would include calculation of the change in entropy associated with the deprotonation process plus calculation of the free enthalpies of solvation of the acidic site, of the conjugate base, and of the proton. J. E. Bartmess[27] showed that the entropy of the deprotonation is nearly independent on the acid/base couple, in the range 100 ± 20 J/mol K. The free enthalpies of solvation can be obtained from molecular dynamics according to the method of W. L. Jorgensen,[28] although with the additional difficulty (with reference to isolated molecules) that the electrostatic environment of the proton near the surface should be reproduced.

One must consider that the prediction of a pK constant with an absolute precision of ±0.5 would imply calculation of the free enthalpy at 300 K with an accuracy of ±3 kJ/mol, which is beyond the capabilities of both Hartree−Fock and molecular dynamics methods. Therefore, the aim of the present work is only to give a physical explanation to the success of simple models giving trends in acidity.

Others quantities calculated were the ω(OH) stretching vibrational frequencies and the electrostatic potential at the acidic proton site $V(\mathbf{r}_H)$.

Results

Test Calculations. A first series of calculations of deprotonation energies has been performed on simple systems involving proton transfer to and from water and from acetic acid (Table 2). The main goal of these calculations is to estimate the relative accuracy of small basis sets (STO-3G) with respect to pseudopotential (ECP LA or ECP ST) or a method using correlated wave functions (MP2/ 6-31G*).

Deprotonation energies are overestimated in all cases. Pseudopotentials give results that compare well with all-electron calculations. Both ECP LA and ECP ST lead to results deviating from experimental data by a range of 80 ± 20 kJ/mol. These conclusions agree with results previously presented by U. Fleischer.[26] The introduction of correlation at MP2 level does not change the results drastically either, while it would make the calculation impossible in practice (considering the memory requirements, CPU time, ...) on the larger systems (sites III and some of the sites II).

TABLE 2: Test Calculations: Deprotonation Energy (kJ/mol)

	H_3O^+/H_2O	ref[a]	H_2O/OH^-	ref[a]	CH_3COOH/CH_3COO^-	ref[a]
Calculation at HF Level, All-Electron						
STO-3G	959	t	2369	t		
3-21G			1881	c		
6-31G*	733	t	1799	t		
Calculation at HF Level, ECP						
ECPLA	761	t	1735	t	1500	t
ECPST	750	t	1662	t		
Calculation Including Correlation						
MP2/6-31G*			1793	c		
G2 (ref e)			1593	a		
experimental	677	b	1635	a	1438	b
experimental	697	d				

[a] References: (a) Acidity and Basicity of Solids, NATO ASI Series C, Vol. 444, p 29. (b) Acidity and Basicity of Solids, NATO ASI Series C, Vol. 444, p 35. (c) Acidity and Basicity of Solids, NATO ASI Series C, Vol. 444, p 46. (d) Fleischer et al. *J. Am. Chem. Soc.* **1993**, *115*, 7833−7838. (e) Curtiss et al. *J. Chem. Phys*. **1991**, 94, 7221. (f) This work.

TABLE 3: Test Calculations on $AlO_4H_5/AlO_4H_4^-$

basis set	calculation	correction	DPE
STO-3G	HF		2446
3-21G	HF		1880
6-31G*	HF		1798
ECP LA	HF		1796
ECP ST	HF		1762
ECP LA	HF		1796
BSSE	HF	−7	1789
ΔE_{zp}	HF	−37	1752
ΔH_{th}	HF	−37	1715
ECP LA	MP2		1736

As another example, the deprotonation of the site Ia on the (110c) surface of δ-alumina has been examined. The physical situation was simulated by a simple AlO_4H_5 cluster which can easily be treated by a post Hartree−Fock method. Comparison of various calculations is illustrated in Table 3: as previously, it demonstrates that pseudopotentials give results comparable to HF/6-31G* and that introduction of the correlation at MP2 level is not necessary.

Calculated Deprotonation Energies on Surfaces Simulated by Clusters. Taking previous results into account, core potential methods have been used to compare calculated deprotonation energies at Brønsted sites of various metal oxides. Oxides of Mg, Al, Si, Ti, Sn, and Ce have been considered, and in each case some cluster models have been chosen to simulate the three different coordinations of the OH group with metals. Typical arrangements are illustrated in Figure 1, and a list of sites and associated clusters is given in Table 1. Table 4 contains the principal results, i.e. calculated deprotonation energies and infrared frequencies ω(OH) of the acidic OH groups.

As exemplified in Figure 2, the two ECP's lead to almost identical values, so we will only display in the following the results of ECP ST that are more general since including CeO_2.

Three factors appear to influence the deprotonation energies: (i) The oxygen coordination number of the OH group

TABLE 4: Deprotonation Energies and IR Frequencies

structure	face	site	deprotonation energy, kJ/mol ECP ST	deprotonation energy, kJ/mol ECP LA	IR, cm^{-1} calc	IR, cm^{-1} attr min	IR, cm^{-1} attr max	ref[a] attr
MgO	100	I	2062	2112	3676	3740	3770	f
	110	II	2001	2043	3708			
	111	III	1840	1880	3669	3690		f
CeO_2	111	I	1875		3639	3710		e
	100	II	1721		3545	3660		e
	111	III	1760		3396	3600		e
SnO_2	110	I	1852	1886	3690	3640		g
Al_2O_3, δ	001	Ib	1928	1971	3715	3745	3800	a, h
	110c	Ia	1704	1796	3814	3760	3800	a, h
	110c	IIb	1719	1744	3804	3710	3745	a, h
	110d	IIa	1541	1565	3535	3710	3735	a, h
	110d	IIIb	1521	1556	3669	3590	3710	a, h
	110c	IIIa	1423	1451	3423	3590		h
Al_2O_3, θ	102	Ia	1755	1783	3855	3760	3780	a
	102	IIIa	1178	1190	3108			
HDO			1662	1735	3668	3707		d
TiO_2, rutile	110	I	1735	1648	3685	3655	3700	c
	110	II	1461	1428	3677	3410	3610	c
	110	III	1377	1388	2942			
TiO_2, anatase	010	I	1639	1541	3654	3725		b
SiO_2 (am)		I	1586	1598	3774	3750		b

[a] References: (a) Knözinger, H.; Ratnasamy, P. *Catal. Rev. Sci. Eng.* **1978**, *17*, 31. (b) Tsyganenko, A. A.; Filimonov, V. N. *J. Molec. Struct.* **1973**, *19*, 579. (c) Rochester, C. H. *Colloids Surf.* **1986**, *21*, 205. (d) Hermansson, K.; Ojamae, L. *Int. J. Quantum Chem.* **1992**, *42*, 1251. (e) Badri, A.; Binet, C.; Lavalley, J. C. To be published in *J. Chem. Soc., Faraday Trans.* (f) Shido, T.; Asakura, K.; Iwasawa, Y. *J. Chem. Soc., Faraday Trans. 1* **1989**, *85*, 441. (g) Harrison, P. G.; Guest, A. *J. Chem. Soc., Faraday Trans. 1* **1987**, *83*, 3383. (h) Busca, G.; Lorenzelli, V.; Sanchez Escribano, V.; Guidetti, R. *J. Catal.* **1991**, *131*, 167.

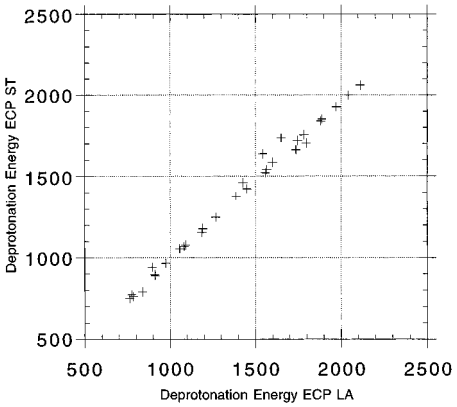

Figure 2. Comparison of the deprotonation energies (kJ/mol) obtained with ECP LA and ECP ST (all materials, all sites, and both first and second deprotonations of site surface$-OH_2^+$).

(sites of type I, II, and III). In Figure 3, the deprotonation energy has been represented as a function of the number of cations coordinated to the oxygen atom of the hydroxyl group. The tendency observed clearly shows that E_d is decreasing when the number of cations increases. This result confirms the prediction made by H. Knözinger[21] and A. A. Tsyganenko[22] on empirical basis who assumed that cations might have an electron-withdrawing effect on the electronic density of the OH group, increasing the polarization of the OH bond. Direct correlation between polarization and acidity has been encountered by organic chemists for a long time.[29]

In particular, the case of aluminum in octahedral coordination is quite illustrative: increasing the coordination number by 1

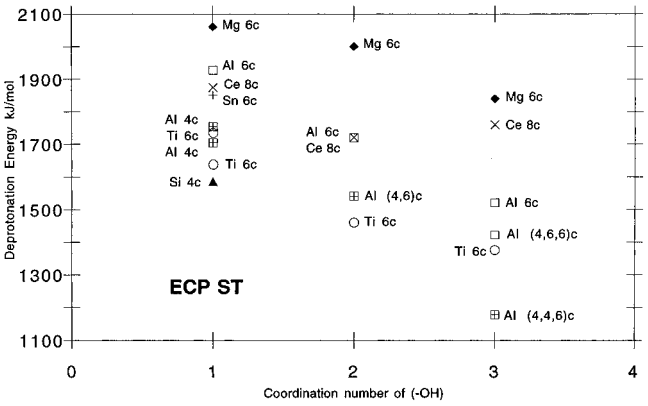

Figure 3. Deprotonation energy (step: surface−OH/surface−O^-) versus coordination number of the OH site. The legend indicates the cation in the oxide, followed by its coordination number in the site. (In the case of alumina, if the site contains several cations in different coordinations, they are explicitly indicated: Al (4,6,6) c refers to a site III in alumina, where one aluminum is in tetraheral coordination and the two others are in octahedral coordination.)

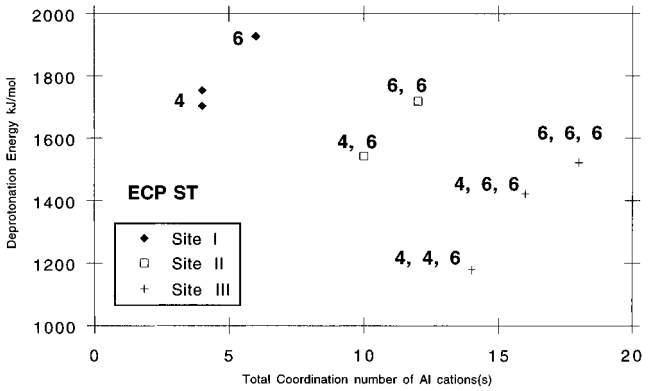

Figure 4. Deprotonation energy (step: surface−OH/surface−O^-) versus coordination number of aluminum in δ- and θ-Al_2O_3. The coordination number of the OH is depicted by the graphism of the point as indicated in the legend, and the coordination numbers of the different Al in the clusters are indicated near the representative points.

unit diminishes E_d by about 200 kJ/mol. Similar results can be found in some of the works of H. Kawakami[30] and E. Knözinger.[31]

(ii) Coordination number of the cation (sites of type a or b). The effect must be studied within a series of materials containing the same cation. As a matter of fact, only aluminum presents two possible coordination numbers, i.e. 4 (tetrahedral) or 6 (octahedral). Any OH site of type I, II, or III could be combined with cations of type a or b, which would generate two, three, or four types of environments for the OH group. However, in fact only some of these cases occur in traditional materials. Thus, in δ-alumina, the OH site environment cannot contain more than one tetrahedral aluminum and sites with three tetrahedral aluminum do not exist in δ- and θ-alumina.

In Figure 4, E_d has been depicted as a function of an overall quantity representing the sum of the coordination numbers of the aluminum atoms bound to the oxygen. It can be deduced from this graph that when the aluminum coordination number decreases from 6 to 4, the proton acidity also decreases by about 200 kJ/mol. Similar arguments to that used when discussing the effect of varying the coordination number of oxygen may again be applied here by considering the metal cation as an electron attractor whose influence is balanced by the electron donor oxygen.

(iii) Nature of the cation. Cation specific effects may be revealed by considering a series of calculations in which the

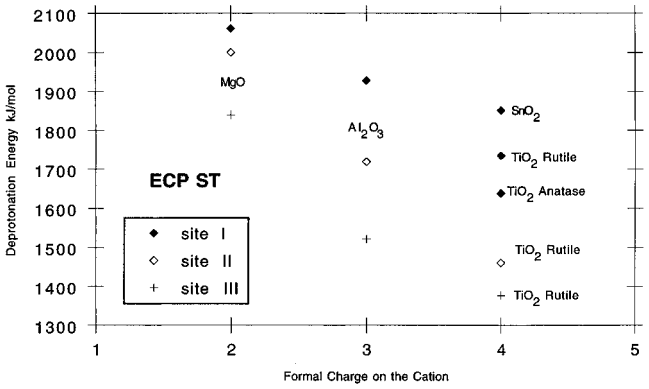

Figure 5. Deprotonation energy (step: surface−OH/surface−O^-) versus formal charge on cation in octahedral site. The coordination number of the OH is depicted by the graphism of the point as indicated in the legend.

TABLE 5: Successive Deprotonations

		ECP LA			ECP ST		
structure	site	first	second	Δ	first	second	Δ
MgO	I	1268	2112	844	1249	2062	813
	II	1186	2043	857	1155	2001	846
CeO_2	I				1245	1875	629
	II				1100	1721	621
Al_2O_3, δ	Ib	1091	1971	881	1077	1928	851
	Ia	894	1796	903	940	1704	764
	IIb	912	1744	832	889	1719	830
	IIa	782	1565	783	761	1541	780
TiO_2, rutile	I	1031	1600	569	1068	1735	667
	II	838	1428	590	789	1461	672
SnO_2	I	1055	1886	831	1055	1852	797
TiO_2, anatase	I	973	1541	569	966	1639	673
SiO_2	I	773	1598	825	772	1586	814
(H_2O)		761	1735	975	750	1662	912

coordination numbers of oxygen and metal cation are kept constant. Variation of E_d is represented in Figure 5 for OH sites in coordination I, II, or III associated to octahedral cation in Al_2O_3, TiO_2, SnO_2, and MgO.

The order of increasing acidity is MgO < Al_2O_3 < TiO_2, and this trend follows the variation of the formal cationic charges.

This order also follows the trends which can be deduced from the few experimental data available[32] and with the general trend assumed in gas phase heterogeneous catalysis.[33]

Calculation of the Proton Affinity PA. It is appropriate to note that calculations on the behavior of hydroxyls are traditionally done in the gas phase by considering the surface−OH/surface−O^- couple. On the other hand, the literature concerning aqueous acid−base chemistry of oxides generally considers two pK_a's: surface−OH_2^+/surface−OH and surface−OH/surface−O^-. For this reason, we considered the two possibilities in most of the calculations, on condition that the oxygen did not become more than 4-fold coordinated.

The results listed in Table 5 show that the "first" acidity (surface−OH_2^+/surface−OH) is stronger that the "second" one (surface−OH/surface−O^-), which agrees with the well-known general trend in polyacids.

The proton affinity values for surface−OH sites are representative of their nucleophilic character. Our results are in agreement with the experimental work.[34]

Calculation of the OH Frequency Mode ω(OH). Results are given in Table 4 and compared to experimentally assigned frequencies. It should be emphasized that assignments to distinct sites are often speculative.

As traditional in HF treatment, the calculated frequencies are above observed values; in order to correct this intrinsic defect,

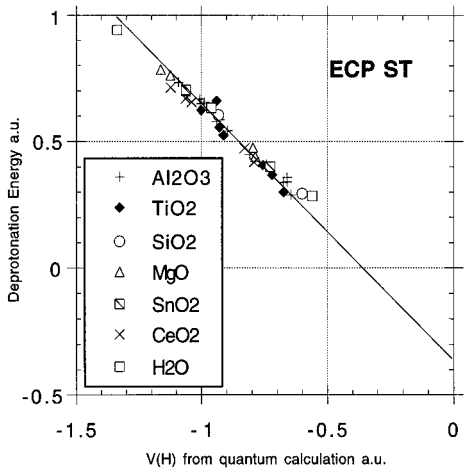

Figure 6. Deprotonation energy versus potential on H (from ab initio wave function) in the acid. au:energy 1 hartree = 2625 kJ/mol, au: potential: 1 au = 27.2 V.

calculated values have been weighted by the factor 0.89.[35] No correction has been attempted to take account for anharmonicity, a factor which would also lower the calculated data and could be important when dealing with vibrational proton motion.

Results gathered in Table 4 support the rule currently accepted of a close correlation between ω(OH) and E_d: the more acidic the site, the lower the ω(OH) frequency. It may be important to emphasize that such a rule has no clear theoretical basis as pointed out by J. A. Lercher.[36] By definition, E_d is related to the height of the dissociation limit with respect to the minimum reached by the potential curve, and ω(OH) is directly given by the curvature at that minimum. Both quantities are mathematically independent though they actually often vary in the same direction.

Furthermore, our results confirm, in general, the attribution of H. Knözinger:[21] the larger the coordination of the oxygen, the lower the frequency.

Calculation of the Electrostatic Potential at the Acidic Proton Site. In the framework of a classical model, the deprotonation energy is interpreted as the energy required to transfer the proton from the site it occupies in the ROH cluster to infinity

$$E_d = E(\infty) - E(\mathbf{r}_H) = 0 - V(H) \times q \qquad (5)$$

where V(H) is the electrostatic potential at $\mathbf{r}_H$ and q the elementary proton charge (q = 1 au). V(H) is deduced from the HF electronic density and directly provided by the GAUSSIAN code. A plot of E_d versus V(H) is displayed in Figure 6. A linear relation is obtained, but an anomalous residual value of −0.35 au persists when V(H) = 0. According to J. Sauer[37] the presence of this term reflects the reorganization of the electronic cloud in the deprotonated cluster. The invariance of the term with the size of the various clusters considered remains unexplained.

Discussion

In the past few decades, many tentative models have been proposed in order to predict Brønsted acidity from structural properties. Most of these models rested on the basic assumption, whether made explicit or not, that acidity is essentially governed by the strength of the electric potential acting on the proton. As we will discuss later, it can be shown that these models can be distinguished by the type of procedure used to approximate the electrostatic potential. Moreover, when treating aqueous solutions, it is assumed that the free enthalpy of proton transfer

to water is linearly related to the potential, the coefficients of the linear transformation being obtained by fitting experimental data: isoelectric points[38,39] or acidity constants.[40]

Before comparing the various models, it is important to point out the physical meaning of the concept of the valence of the electrostatic bond introduced by Pauling[41] and later used by many authors as partial charges. Let there A_aB_b be a binary ionic crystal where A and B are the cation and anion, respectively. The constraint of electrical neutrality imposes the condition

$$aq_A + bq_B = 0 \tag{6}$$

where q_A and q_B are the charges on cation and anion and a and b are the stoichiometric coefficients, but no additional conditions are imposed on the coordination numbers CN_A and CN_B.

On the other hand, the electrostatic potential at some arbitrary point chosen as origin is given by a Madelung-type summation

$$V = \sum_{i \in \text{crystal}} \frac{q_i}{|\mathbf{r}_i|} \tag{7}$$

where the summation is extended to all ions i located at sites $\mathbf{r}_i$ and bearing a formal charge q_i. In order to obtain a convergent sum, M. Adamowicz[42] proposed to associate charges in identical clusters, each one representing one cation and its shell of nearest anions. By construction, each anion belongs to CN_B clusters, and the charge conservation requirement imposes that it contributes an amount of charge to each cluster equal to q_B/CN_B. Then (7) can be reorganized as

$$V = \sum_m \left(\frac{q_A}{|\mathbf{r}_m|} + \sum_j \frac{q_B}{CN_B} \frac{1}{|\mathbf{r}_m + \mathbf{r}_j|} \right) \tag{8}$$

where suffix m runs over cations, j runs over the CN_A nearest anions, $\mathbf{r}_m$ is the position vector of a cation, and $\mathbf{r}_j$ connects a cation to its nearest anion. Since $|\mathbf{r}_j| \ll |\mathbf{r}_m|$, each term of the summation present in (8) can be expanded in a Taylor series to yield the multipolar representation of the corresponding cluster.

The zero-order term will be

$$V_0 = \left(q_A + CN_A \frac{q_B}{CN_B} \right) \sum_m \frac{1}{|\mathbf{r}_m|} \tag{9}$$

In order to ensure that the potential V_0 remains finite when the size of the solid is increased ($m \rightarrow \infty$), the charge term must be zero.

This is proof of the second building rule of L. Pauling,[41] ($q_A/CN_A = -q_B/CN_B = \upsilon$), which was first introduced as a postulate.

These latter considerations, which are relevant for a three-dimensional bulk, are no longer valid when applied to a sample limited in one direction by a two-dimensional surface. The partition of charges contained in the volume and on the surface is incomplete due to the truncation of summations in one direction. As a result, the surface charges are partitioned into charged multipole moments where summation on the two-dimensional surface gives rise to difficulties which have not yet been overcome.

The net effect of these surface charges or multipoles is to create at any point ($\mathbf{r}'$) above the surface an electric potential $V(\mathbf{r}')$ and electric field $E(\mathbf{r}')$. This field may be simulated by a charge q or a set of charges (q_i) located at some distance R (respectively R_i) from the surface chosen, so that $V(\mathbf{r}') = q/R$ or $V(\mathbf{r}') = \sum_i (q_i/R_i)$. Using the theory of image charges, the charge q can be chosen at a position symmetrical to $\mathbf{r}'$ with respect to the surface. In the literature on surface acidity, there is a routine practice consisting of placing the charges on the atomic positions nearest to the hydroxyl, an assumption which implies (i) neglect of all effects arising from multipolar clusters except from the one attached to the site and (ii) use of a simplified model for this multipole.

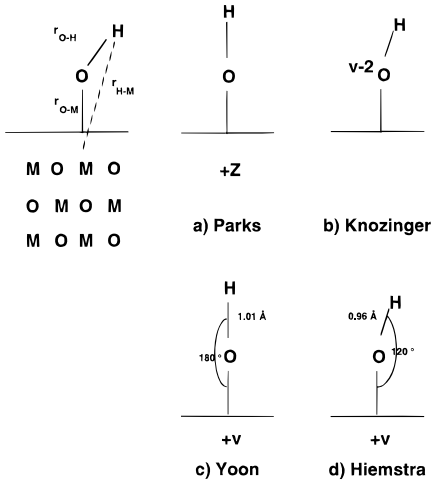

Figure 7. Surface hydroxyl on a solid and its simplified electrostatic simulations in classical models. In each case, r_{O-M} is supposed to be equal to the O−M distance in the bulk crystal.

Among the most representative models, four types may be distinguished (as exemplified in Figure 7):

(i) The ionic pair model is the crudest model introducing some specificity of the surface. The system is reduced to the interaction of the hydroxyl group with a metal cation. In this approach, proposed by Parks,[38] the potential at the proton site is given by

$$V(\text{H}) = \frac{-2}{r_{O-H}} + \frac{Z_M}{r_{H-M}} \tag{10}$$

(The notations for distances are detailed in Figure 7a; Z_M is the formal charge on the cation.)

(ii) The perturbed site consisting of one cation and $CN_M - 1$ anions can also be represented at zero order by a charge $\upsilon = Z_M - (CN_M - 1)(Z_M/CN_M) = Z_M/CN_M$ located at the site of the missing coordinant, i.e. at the position of the oxygen in the hydroxyl. The potential at H becomes (Figure 7b)

$$V(\text{H}) = \frac{-2}{r_{O-H}} + \frac{\upsilon}{r_{O-H}} \tag{11}$$

This is equivalent to modifying the charge at the oxygen site. This is the basic ingredient of the qualitative model of H. Knözinger.[21]

(iii) In the model proposed by R. H. Yoon,[39] the charge term is placed rather in the cationic position. The V(H) potential is then given by (Figure 7c)

$$V(\text{H}) = \frac{-2}{r_{O-H}} + \frac{\upsilon}{r_{H-M}} \tag{12}$$

(iv) If several (n) surrounding cations are taken into account, (11) is the basic equation of the MUSIC model proposed by T. Hiemstra[40] (Figure 7d):

$$V(\text{H}) = \frac{-2}{r_{O-H}} + \frac{n\upsilon}{r_{H-M}} \tag{13}$$

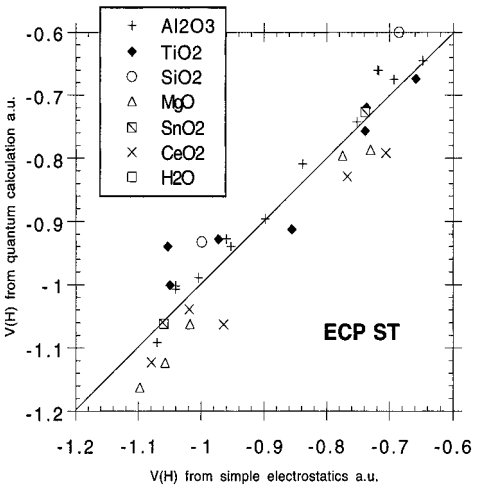

Figure 8. Potential on H from ab initio wave function versus potential on H from simple electrostatics. au:potential 1 au = 27.2 V.

The results obtained with these formulas can be correlated to the quantum mechanical calculations reported above by calculating (with the GAUSSIAN code) the electrostatic potential $V(H)$ in the acidic proton position. In Figure 8, the $V(H)$ potentials from ab initio calculation are compared to results deduced from the empirical formula

$$V(\mathrm{H}) = \frac{-2}{r_{\mathrm{O-H}}} + \frac{n\upsilon}{r_{\mathrm{H-M}}}b \qquad (14)$$

in the case of deprotonation of a single protonated site (surface−OH ⟹ surface−O^-) and

$$V(\mathrm{H}) = \frac{-2}{r_{\mathrm{O-H}}} + \frac{n\upsilon}{r_{\mathrm{H-M}}}b + \frac{1}{r_{\mathrm{H-H}}} \qquad (15)$$

when the acidic site is twice protonated (surface−OH_2^+ ⟹ surface−OH).

Calculations performed with parameters resulting from optimized geometry and optimization by a least-squares procedure lead to $b = 0.626$ and a root mean square error less than 5%.

Using the mean values $r_{\mathrm{O-H}} = 1.758$ au, $r_{\mathrm{H-H}} = 3.027$ au, and $r_{\mathrm{H-M}} = 7.51$ au instead provides a root mean square error of 7%, with the same value of b. This supports our hypothesis of neglecting the effects of surface reconstruction and geometry relaxation on the cation during deprotonation.

It is remarkable that the b value of 0.626 is close to the ratio of the partial charge from electrostatic potential fitting (CHELPG algorithm[23]) on the formal charge of the clusters. This shows that, while the formal charge is representative of the electrostatics at short range (O−H, H−H), the charges from ESP fit are more representative of the long-range effect.

The agreement between the two approaches, quantum mechanical and empirical, and their ease of reproducing experimental trends confirm that local approximations are good models for simulation of surface long-range effects. A definitive explanation of this property would demand a careful analysis of two-dimensional summation of charges or charged multipoles over the surface. Cancellations of terms within infinite summations is a possible explanation.

The above discussion assumed that the surface is infinite in both directions and perfectly planar, but these conditions are rarely satisfied on experimental surfaces: various defects (boundary conditions, steps, dislocations, ...) may be at the origin of inhomogeneities in the field acting on the proton. The representation of these defects could be of much greater importance for reproducing the exact field than a more sophisticated representation of an averaged field resulting from a hypothetical perfect surface.

Conclusion

Ab initio calculations on clusters simulating surface sites of silica, titanium dioxide, tin oxide, alumina, ceria, and magnesia have emphasized the determining role of the structural parameters (coordination, charge) on the evaluation of surface acidity.

Also, these calculations support and justify the relative success of simple electrostatic models, which permit evaluation of deprotonation energies with an accuracy of about 10% compared to the exact (Hartree−Fock) values.

Finally, in relation to these results the physical origin of the rule stated by L. Pauling on the strength of the electrostatic bond has been reexamined and used to present the common origin of the different models of surface acidity and to show why they can qualitatively provide a reasonable estimation of surface electrostatic effects.

Acknowledgment. The authors thank J. C. Lavalley, P. Hoggan, and M. A. Perrin for helpful discussions. This work was supported by Rhône-Poulenc, Chemical Division.

References and Notes

(1) Hiemstra, T.; de Wit, J. C. M.; Van Riemsdijk, W. H. *J. Colloid Interface Sci*. **1989**, *131*, 105. Hiemstra, T.; Van Riemsdijk, W. H. *J. Colloid Interface Sci*. **1996**, *179*, 488. Venema, P.; Hiemstra, T.; Van Riemsdijk, W. H. *J. Colloid Interface Sci*. **1996**, *181*, 45.

(2) Henry, M. Soft Chemistry Routes to New Materials. Int. Symp. Nantes, France, Sept 6−10, 1993.

(3) Contescu, C.; Contescu, A.; Schwarz, J. A. *J. Phys. Chem.* **1994**, *98*, 4327.

(4) Pisani, C.; Dovesi, R. *Int. J. Quantum Chem*. **1980**, *17*, 501. Pisani, C.; Dovesi, R.; Roetti, C. In *Lecture Notes in Chemistry 48*; Berthier, G., Dewar, M. J. S., Fisher, H. K., Fukui, K., Hall, G. G., Hinze, J., Jaffe, H. H., Jortner, J., Kutzelnigg, W., Ruedenberg, K., Thomas, J., Eds.; Springer: Heidelberg, Germany, 1988. Silvi, B.; Fourati, N.; Nada, R.; Catlow, C. R. A. *J. Phys. Chem. Solids* **1991**, *52*, 1005. Hill, S. E., Catlow, C. R. A. *J. Phys. Chem. Solids* **1993**, *54*, 411.

(5) Pisani, C.; Dovesi, R.; Nada, R.; Kantorovich, L. N. *J. Chem. Phys*. **1990**, *92*, 7448.

(6) Zhidomirov, G. M.; Kazansky, V. B. *Adv. Catal*. **1986**, *34*, 131 and references cited therein.

(7) Seiti, K.; Kassab, E.; Allavena, M. *J. Phys. Chem*. **1991**, *95*, 9425.

(8) Sauer, J. *Chem. Rev*. **1989**, *89*, 199.

(9) Fleischer, M. B.; Golender, L. O.; Shimanskaya, M. V. *React. Kinet. Catal. Lett*. **1992**, *46*, 173.

(10) Gorb, L. G.; Gunko, V. M.; Goncharuk, V. V.; Karakhim, S. A. *React. Kinet. Catal. Lett*. **1989**, *38*, 21.

(11) Fahmi, A. Ph.D. Thesis, Univ. Pierre et Marie Curie, Paris, France, 1993.

(12) Bagou, F.; Bigot, B.; Sautet, P. *J. Phys. Chem*. **1993**, *97*, 11501.

(13) Pacchioni, G.; Cogliandro, G. *Surf. Sci*. **1991**, *255*, 344.

(14) Zhixing, C.; Zhengwu, W.; Ruiyu, H.; Yala, Z. *J. Catal*. **1983**, *79*, 271.

(15) Fleischer, M. B.; Golender, L. O.; Shimanskaya, M. V. *React. Kinet. Catal. Lett*. **1992**, *46*, 73. Hirva, P.; Pakkanen, T. A. *Surf. Sci*. **1992**, *277*, 389. Lindblad, M.; Pakkanen, T. A. *Surf. Sci*. **1993**, *286*, 333. Manassidis, I.; De Vita, A.; Gillan, M. J. *Surf. Sci. Lett*. **1993**, *285*, L517. Hagfeldt, A.; Siegbahn, H.; Lindquist, S. E.; Lunell, S. *Int. J. Quantum Chem*. **1992**, *44*, 477.

(16) Cerius 3.1, Molecular Simulations Inc., 1992.

(17) Insight II, version 2.3.0, Biosym Technologies, San Diego, 1993.

(18) Repelin, Y.; Husson, E. *Mater. Res. Bull.* **1990**, *25*, 611 and personal communication.

(19) Gay, D. H.; Rohl, A. L. *J. Chem. Soc., Faraday Trans.* **1995**, *91*, 925

(20) Pisani, C.; Causa, M.; Dovesi, R.; Roetti, C. *Prog. Surf. Sci.* **1987**, *25*, 119

(21) Knozinger, H.; Ratnasamy, P. *Catal. Rev.—Sci. Eng*. **1978**, *17*, 31.

(22) Tsyganenko, A. A.; Filimonov, V. N. *J. Mol. Struct*. **1973**, *19*, 579.

(23) Frisch, M. J.; Trucks, G. W.; Head-Gordon, M.; Gill, P. M. W.; Wong, M. W.; Foresman, J. B.; Johnson, B. G.; Schlegel, H. B.; Robb, M. A.; Replogle, E. S.; Gomperts, R.; Andres, J. L.; Raghavachari, K.; Binkley, J. S.; Gonzalez, C.; Martin, R. L.; Fox, D. J.; Defrees, D. J.; Baker, J.; Stewart, J. J. P.; Pople, J. A. *Gaussian 92*, Revision D.2; Gaussian, Inc.: Pittsburgh, PA, 1992.

(24) Hay, P. J.; Wadt, W. R. *J. Chem. Phys*. **1985**, *82*, 270, 284, 299.
(25) Dolg, M.; Stoll, H.; Preuss, H. *J. Chem. Phys*. **1989**, *90*, 3. Dolg, M.; Stoll, H.; Savin, A.; Preuss, H. *Theor. Chim. Acta* **1989,** *75*, 173. Dolg, M.; Stoll, H.; Preuss, H. *Theor. Chim. Acta* **1993**, *85*, 441. Dolg, M.; Wedig, U.; Stoll, H.; Preuss, H. *J. Chem. Phys*. **1987**, *86*, 866.
(26) Fleischer, U.; Kutzelnigg, W.; Bleiber, A.; Sauer, J. *J. Am. Chem. Soc.* **1993**, *115*, 7833.
(27) Bartmess, J. E.; Scott, J. A.; McIver, R. T., Jr. *J. Am. Chem. Soc.* **1979**, *101*, 6046.
(28) Jorgensen, W. L.; Briggs, J. M. *J. Am. Chem. Soc.* **1989**, *111*, 4190.
(29) March, J. *Advanced Organic Chemistry*, 2nd ed.; Mc Graw-Hill: New York, 1977; p 238.
(30) Kawakami, H.; Yoshida, S. *J. Chem. Soc., Faraday Trans.* **1986**, *82*, 1385.
(31) Knozinger, E.; Jacob, K-H.; Singh, S.; Hofmann, P. *Surf. Sci.* **1993**, *290*, 388.
(32) Auroux, A.; Gervasini, A. *J. Phys. Chem*. **1990**, *94*, 6371.
(33) Tanabe, K. *Solid acids and bases, their catalytic properties*; Academic Press: New York, 1970.
(34) Lavalley, J. C. *Catal. Today* **1996**, *27*, 377.
(35) Pulay, P.; Fogarasi, G.; Pongor, G.; Boggs, J. E.; Vargha, A. *J. Am. Chem. Soc*. **1983**, *105*, 7037. Hess, B. A.; Schaad, L. J.; Carsky, P.; Zahradnik, R. *Chem. Rev*. **1986**, *86*, 709.
(36) Lercher, J. A.; Grundling, C.; Eder-Mirth, G. *Catal. Today* **1996**, *27*, 353.
(37) Sauer, J.; Ahlrichs, R. *J. Chem. Phys*. **1990**, *93*, 2575.
(38) Parks, G. A. *Chem. Rev*. **1965**, *65*, 177.
(39) Yoon, R. H.; Salman, T.; Donnay, G. *J. Colloid Interface Sci*. **1979**, *70*, 483.
(40) Hiemstra, T.; de Wit, J. C. M.; van Riemsdijk, W. H. *J. Colloid Interface Sci*. **1989**, *131*, 105.
(41) Pauling, L.*The Nature of the Chemical Bond*; Cornell University Press: Ithaca, NY, 1948.
(42) Adamowicz, M.; Lalauze, R.; Vernay, A. M.; Soustelle, M. *J. Chim. Phys*. **1970**, *67*, 1928.